Bioactivity of Nanohybrid: Comprising of Metallosalen Incorporated into Lacunary Polyoxometalate and Encapsulated with Chitosan Biopolymer

SHIVA ARUN[a], VINAY KUMAR SINGH[a#], PRABHA BHARTIYA[b], AND PRADIP KUMAR DUTTA[c*]

[a]*Department of Chemistry, Dr. Shakuntala Misra National Rehabilitation University, Lucknow-226017, India.*

[b]*Department of Chemistry, Sant Ganinath Government PG College, Muhammadabad Gohna, Mau-276403, India.*

[c]*Department of Chemistry, Motilal Nehru National Institute of Technology Allahabad, Prayagraj-211004, India.*

[#] *Present Address: Department of Chemistry, University of Lucknow-226007, India.*

ABSTRACT

Biocompatible polymer chitosan has note-worthy applications in biomedical science. Nanohybrids synthesized by using chitosan as an encapsulating unit for polyoxometalates (POMs) and study of its biomedical applications is a fast-emerging field. In this research work, a lacunary polyoxometalate (α-$K_8SiW_{11}O_{39}$) has been synthesized and then alkylsilane has been inserted into its lacunary position. It has been then reacted with 2-hydroxy-1-naphtaldehyde followed by copper metalation and finally encapsulated into chitosan by using the ionotropic gelation technique, in which the chitosan and the POM served as cation and anion, respectively. The bands in UV-Vis spectra at characteristic wavelength indicate that the organosilane is successfully inserted into α-$K_8SiW_{11}O_{39}$ and metalled with Cu. Then its encapsulation into chitosan to synthesize final nanohybrid has been confirmed by UV-Vis spectra. Further, chitosan, POM inserted with organosilane and nanohybrid have been characterized by FT-IR. EDX analysis reveals the presence of all the expected elements in their desired ratios. EDX study was further supported by Inductively Coupled Plasma (ICP) technique. Morphology of nanohybrid has been studied by Scanning Electron Microscope (SEM) imaging. The loading and entrapment efficiency

J. Polym. Mater. Vol. **40,** No. 1-2, 2023, 19-31

*Correspondence author e-mail: pkd@mnnit.ac.in
DOI : https://doi.org/10.32381/JPM.2023.40.1-2.2

of the prepared nanohybrid was exceptionally excellent and was calculated to be 81.2% and 59.1%, respectively. In vitro drug release study suggested sustainable and pH-modulated release behaviour of the nanohybrid. Further, it is the first time that an organosilane attached to lacunary POM, then metalated with Cu and finally encapsulated into CS has been investigated for drug delivery. The antibacterial activity of POM inserted with organosilane and nanohybrid have been tested against bacterial strains of B. subtilis gram (+)ve and E. coli gram (-)ve. The antibacterial activity of nanohybrid has been improved as compared to bare POM inserted with metallated organosilane and chitosan.

KEYWORDS: *Metallosalen, Chitosan, Organosilane, Nanohybrid, Bioactivity.*

1. INTRODUCTION

Chitin is biodegradable polysaccharide which is obtained from shrimp's exoskeleton and shells of crustacean, further the N-deacetylation of chitin produce chitosan (CS)[1]. CS occurs in nature in abundant amount and provides high degree of biocompatibility including antibacterial, antifungal and wound healing properties[2]. In human body, biocompatible CS has been extensively studied for transport of various vaccines, drugs and genes[3].

Polyoxometalates (POMs) are well known class of stable oxoclusters with transition metal (generally Mo, V, W) which offer variety in size and composition, therefore POMs have drawn attention for applications in diverse spectrum of luminescent, catalytic, magnetic, biomedical, dye degradation and other properties.[4] Research on POM-based systems increased because they have been proved as an important tool for application in antibacterial, antiviral and anticancer activities[5]. The lacunary position of POM can be exploited to synthesize various hybrids having versatile properties and applications.[6]

Encapsulation of POMs possessing bioactivity into biodegradable CS polymer, offer various avenues for development of drugs [7-8] having greater stability at different pH [9], high potential bioactivity with reduced toxicity and effective bio-distribution[10].

In the present research communication firstly a stable lacunary POM molecule ($K_8[SiW_{11}O_{39}].13H_2O$) (LPOM) has been synthesized from its saturated parent compound ($K_8[SiW_{12}O_{40}].xH_2O$) by releasing one tungstate unit[11]. LPOM molecule has a 'cavity' called 'lacunary hole' which has been substituted by organosilane3-(Triethoxysilyl) propylamine (LPOM-Sil). Further it was reacted with 2-hydroxy-1-naphtaldehyde to form LPOM-Sil-HN and then metalated with copper to synthesize LPOM-Sil-HN-Cu. Copper metalation of LPOM-Sil-HN has been performed to enhance the antibacterial property. LPOM-Sil-HN-Cu has been encapsulated into CS to give final nanohybrid (NHyd). NHyd has exhibited excellent loading and entrapment efficiency. Drug release study suggested their potential application for pH-dependent sustained release for tumor therapeutics. LPOM-Sil-HN-Cu and NHyd have been tested against bacterial strains of *B. subtilis* gram(+)ve and *E. coli* gram (-)ve respectively.

2. EXPERIMENTAL

2.1 Materials and Characterization Techniques

CS (low molecular weight), silicotungstic acid $H_4[SiW_{12}O_{40}].xH_2O$, Copper acetate anhydrous, tetrahexylammonium bromide, 3-(Triethoxysilyl) propylamine, 2-hydroxy-1-naphthaldehyde, and trimethylorthoformate (A.R. grade) were purchased from sigma and used without further purification. Potassium bicarbonate, acetic acid, ethanol have been purchased from CDH and are of A.R. grade. Nutrient broth and Nutrient agar have been purchased from Titan Biotech Ltd. Rajasthan, India. The test strain *B. subtilis* gram(+)ve. bacteria and *E.coli* gram (-)ve bacteria have been obtained from IMTECH, Chandigarh, India. FT-IR spectra have been recorded in the range of wave number 4000–300 cm^{-1} using KBr disks with Perkin Elmer spectrophotometer. For detecting the elemental composition of hybrid EDX detector coupled with Nova Nano FE-SEM 450 (FEI) has been used. Shimadzu UV-2450 has been used to record UV–visible spectra. ICP-AES analysis has been performed by SPECTRO Analytical Instruments GmbH-ARCOS, Simultaneous ICP Spectrometer.

2.2 Preparation of LPOM

LPOM (Fig. 1) has been synthesized by the reported procedure of Tézé and Hervé[11]. FT-IR (cm^{-1}, KBr): 536, 710, 742, 797, 852, 870, 909, 950.

2.3 Incorporation of Organosilane into Lacunary Position of LPOM to Synthesize LPOM-Sil

Following the procedure of Bar-Nahum et al., [12], firstly organosilane {3-(Triethoxysilyl)propylamine $(C_2H_5\text{-}O)_3\text{-}Si\text{-}(CH_2)_3\text{-}NH_2\cdot HCl$} has been functionalized, followed by incorporation at the lacunary position of LPOM(scheme 1), thus forming $\{SiW_{11}O_{39}[O(Si\text{-}CH_2\text{-}CH_2\text{-}CH_2\text{-}NH_2\cdot HCl)_2]\}^{4-}$. Tetrahexylammonium bromide has been added to attain tetrahexylammonium $(n\text{-hexyl})_4N^+$ salt of LPOM-Sil i.e. $Q_4\{SiW_{11}O_{39}[O(Si\text{-}CH_2\text{-}CH_2\text{-}CH_2\text{-}NH_2\cdot HCl)_2]\}$, (Q = $(n\text{-hexyl})_4N^+$). FT-IR(cm^{-1}, KBr): 535, 710, 741, 794, 852, 870, 910, 954, 1045, 1155, 1232, 1482, 2948, 3240, 3445.

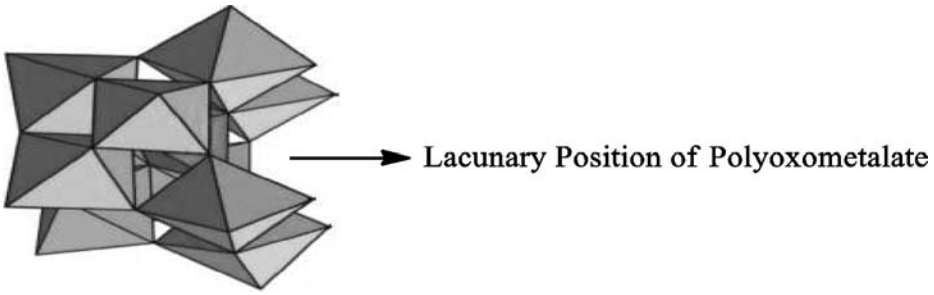

Fig. 1. Lacunary Polyoxometalate ($K_8[SiW_{11}O_{39}].13H_2O$) (LPOM)

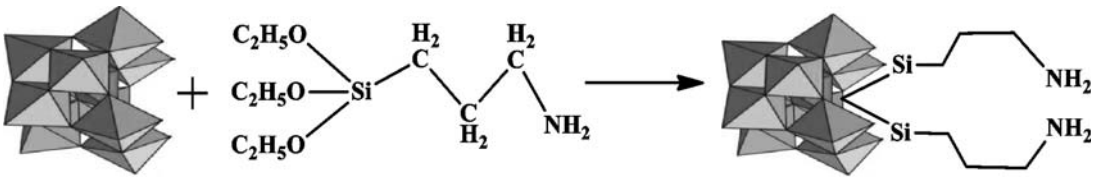

Scheme 1. Schematic presentation for synthesis of LPOM-Sil by incorporation of organosilane into LPOM

2.4 Synthesis of LPOM-Sil-HN by Attachment 2-Hydroxy-1-Naphthaldehyde to LPOM-Sil

Further, 2-hydroxy-1-naphthaldehyde, has been attached to $Q_4\{SiW_{11}O_{39}$-[O-(Si-CH_2-CH_2-CH_2-NH_2.HCl)$_2$]} to synthesize $Q_4\{SiW_{11}O_{39}$[O-(Si-CH_2-CH_2-CH_2-N=CH(2-OH-Naph)$_2$]}(LPOM-Sil-HN)[13]. 2-hydroxy-1-naphthaldehyde 0.735 gm (0.42 mmol) has been dissolved in absolute methanol then salts of LPOM-Sil 0.9 gm (0.21 mmol) has been added and continuously stirred for 24 hours at 25°C (±1°C) (Scheme 2). To this mixture trimethylorthoformate (8ml) was added as drying agent and stirred overnight at 25°C (±1°C). Light yellow colored precipitate was obtained which was filtered and washed with dry either several times. FT-IR(cm^{-1}, KBr): 534, 710, 741, 795, 850, 872, 910, 953, 1045, 1156, 1230, 1481, 1614, 1632, 2946, 3241, 3446.

2.5 Metalation of LPOM-Sil-HN

Same metalation procedure was followed as reported by Bar-Nahum et al.,[12] for the synthesis of LPOM-Sil-HN-Cu (Scheme 3). For the synthesis of LPOM-Sil-HN-Cu, 1.5 g (0.32 mmol) of LPOM-Sil-HN was dissolved in degassed DMF (5mL) and heated to 70°C in inert atmosphere of argon with constant stirring (Scheme 3). A solution of 0.32 mmol of copper acetate anhydrous in DMF were added to the above solution and maintained at 70°C (±1°C) for 45 min before being cooled to 25°C (±1°C). Methanol (30mL) was added, and the precipitate was filtered and washed thoroughly with methanol and ether before vacuum drying. CHNO elemental analysis for LPOM-Sil-HN-Cu (Chemical formula: $C_{28}H_{30}CuN_2O_{42}Si_3W_{11}$; Mol. Wt.: 3236.57; Greenish blue color) calculated % C, 10.34; H, 0.90; N, 0.83; O, 20.70; found % C, 10.36; H, 0.91; N, 0.84; O, 20.72.

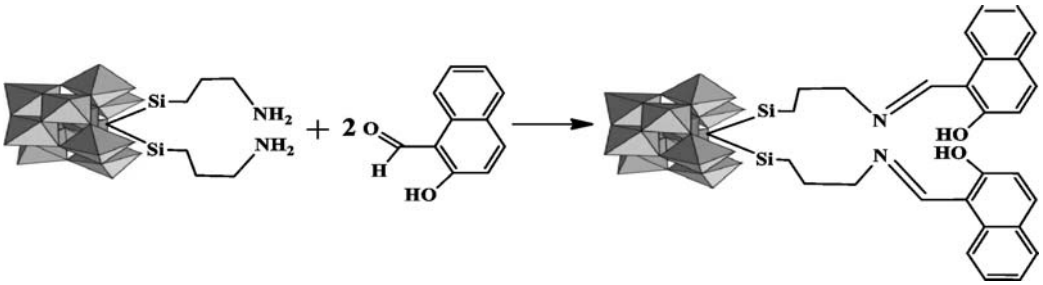

Scheme 2. Schematic presentation of Metalation of 2-hydroxy-1-naphthaldehyde attached to LPOM-Sil

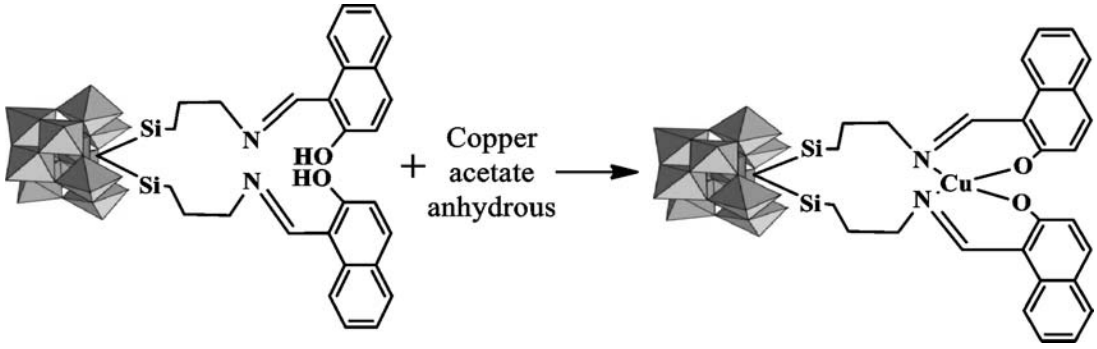

Scheme 3. Schematic presentation of Metalation of LPOM-Sil-HN with Copper Acetate Anhydrous to synthesize LPOM-Sil-HN-Cu

2.6 Synthesis of NHyd by Encapsulation of LPOM-Sil-HN-Cu into CS matrix

NHyd has been prepared using the ionotropic gelation technique by previously reported method, in which the chitosan and the POM served as cation and anion, respectively [5(c)]. In order to synthesize NHyb comprising of CS and LPOM-Sil-HN-Cu (Scheme 4), CS has been dissolved in 2% v/v acetic acid to give concentrations of 0.50% w/v. The CS solution filtered to remove any suspended particles and heated at 50°C for 2 hours with continuous stirring and then cooled to room temperature (Solution 1). pH of above solution (Solution1) has been maintained at 6.5 with NaOH. 0.1 gm of LPOM-Sil-HN-Cu dissolved in minimum amount of milli-Q water (Solution 2). Solution 2 has been added to Solution1 drop-wise under the controlled sonication for 10 minutes resulting into a stable colloidal suspension of LPOM-Sil-HN-Cu and CS nano-hybrid which is hereafter abbreviated as NHyd. This colloidal suspension containing NHyd was stirred at room temperature for 10 hours (h) and then centrifuged for 20 minutes (min), at 20,000 rpm to collect NHyd. The NHyd of CS and LPOM-Sil-HN-Cu was collected and washed with milli-Q water several times and dried under vacuum.

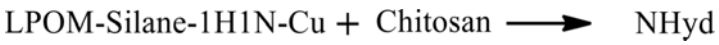

Scheme 4. Schematic presentation for synthesis of NHyd by encapsulation of LPOM-Sil-HN-Cu into CS

2.7 Entrapment and Loading Studies

The entrapment and loading efficiency of NHyd was determined by spectrophotometrically as described by Menon et al., [14]. Briefly, known amount of NHyd was dispersed in Milli-Q water and further centrifuged at 10,000 rpm for 30 min and the supernatant collected was analyzed under UV-visible spectrophotometer to quantify the amount of non-entrapped LPOM-Sil-HN-Cu in the NHyd by using the following formula:

$$\textit{Entrapment Efficiency}\ (\%) = \frac{\textit{Total}\ \text{LPOM} - \text{Sil} - \text{HN} - \textit{Cu conc. in Nhyd} - \text{Free LPOM} - \text{Sil} - \text{HN} - \text{Cu}}{\textit{Total}\ \text{LPOM} - \text{Sil} - \text{HN} - \textit{Cu conc. in Nhyd}} \times 100$$

$$\textit{Loading Efficiency}\ (\%) = \frac{\textit{Total}\ \text{LPOM} - \text{Sil} - \text{HN} - \textit{Cu conc. in Nhyd}}{\textit{Total Weight of Nhyd}} \times 100$$

2.8 *In Vitro* Release of LPOM-Sil-NH-Cu from NHyd

The *in vitro* release study of LPOM-Sil-HN-Cu from NHyd, was investigated at 37°C in two different pH (7.4 & 5.0) of phosphate buffer saline (PBS) by following a previously reported method [15]. Predetermined weight of NHyd was dispersed in 10mL PBS and was transferred to dialysis bag (MW cut off: 12kDa). The dialysis bag was immersed in 50mL of PBS kept on orbital shaker. At predetermined intervals, 2mL aliquot was taken out and was compensated with fresh PBS. The standard curve for POM was used to determine its time dependent release profile.

2.9 Antibacterial Study

The antibacterial study of prepared NHyd and bare LPOM-Sil-HN-Cu was performed against two bacterial strains namely *B. subtilis* gram (+) ve and *E. coli* gram (-) ve. Antibacterial test was performed by agar diffusion method as described by P. Bhartiya et al., [16]. The inoculum of bacterial strains was prepared from the fresh overnight culture in sterilized Nutrient Broth (13 g/L) by incubation at 37°C. The diffusion technique was performed by pouring sterilized nutrient agar into petri dishes and left for drying. Subsequently, the active broth culture of each bacterial strain (1% of the bacterial culture in order to obtain 105 CFU mL^{-1}). Inoculated agar

plates were treated with bare LPOM-Sil-NH-Cu and NHyd in 100µl of aqueous solution and put in wells (8 mm) with control (water). The incubation was continued overnight at 37°C, and finally the zone of inhibition (diameter) was measured in (mm) to determine the antibacterial efficacy.

3. RESULTS AND DISCUSSION

3.1 FT-IR spectra

Appearance of similar FT-IR (cm^{-1}) bands (Fig. 2a) as reported in reference [12] confirmed the formation of (α-$K_8SiW_{11}O_{39}$). Successful incorporation of organosilane $Q_4\{SiW_{11}O_{39}$-$[O(Si\text{-}CH_2\text{-}CH_2\text{-}CH_2\text{-}NH_2.HCl)_2]\}$ into the lacunary position of (α-$K_8SiW_{11}O_{39}$) for the formation of LPOM-Silane has been confirmed by the occurrence of FT-IR bands (Fig. 2b) at 1045 (υ_{asym} Si-O-Si), 1155 (C-N), 1232(Si-C), 1482 (C-H), 2948 (C-H), 3240 (N-H), 3445 (N-H) along with LPOM peaks at 710 (υ_{asym} WOW), 741 (υ_{asym} WOW), 797 (υ_{asym} WOW), 852 (υ_{asym} WOW), 870 (υ_{asym} WOW), 910 (υ_{asym} W=O), 955 (υ_{asym} W=O). Earlier workers have reported similar FT-IR behaviour [6]. Covalent attachment of 2-hydroxy-1-naphthaldehyde through the C

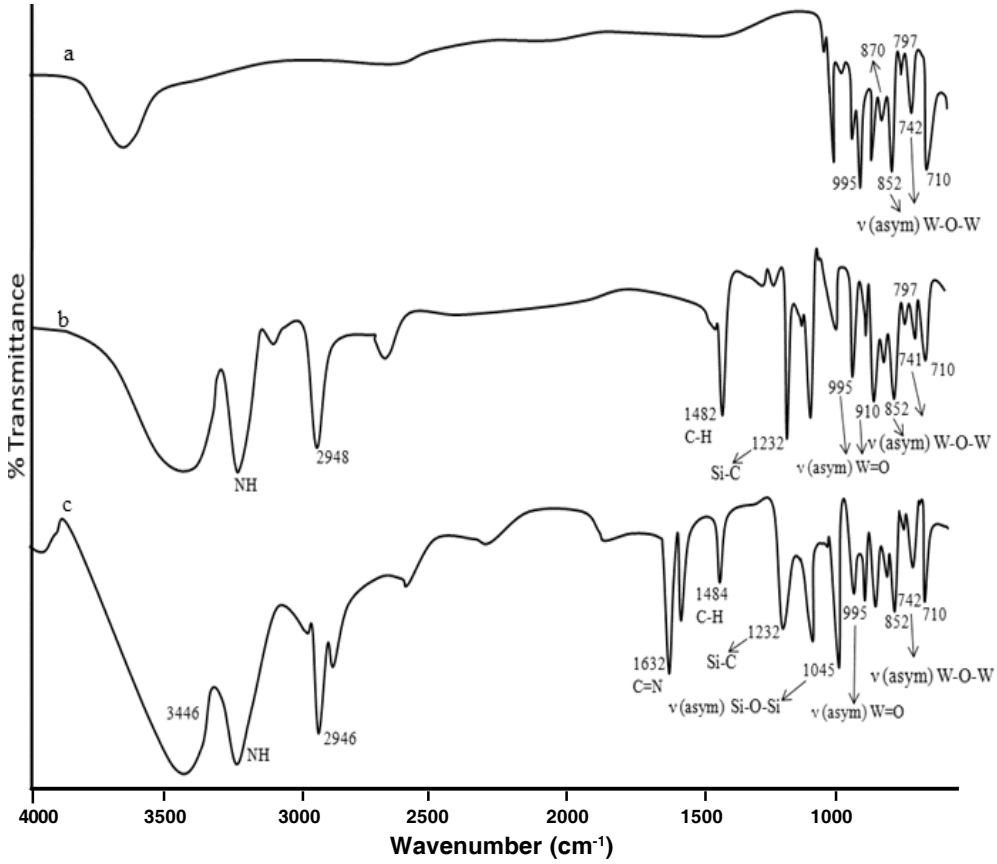

Fig. 2. FT-IR (a) α-$K_8SiW_{11}O_{39}$; (b) LPOM-Sil; (c) LPOM-Sil-HN

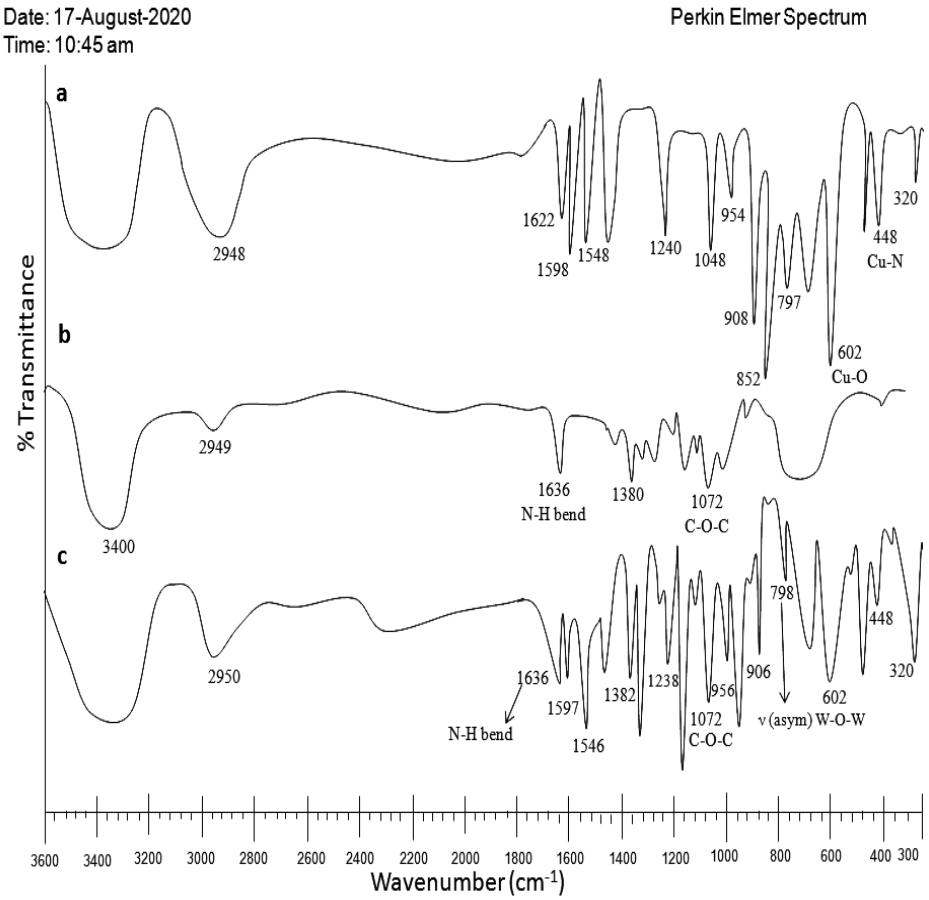

Fig. 3. (a) LPOM-Sil-HN-Cu (b) CS (c) NHyd

atom of carbonyl group to N atom of organosilane has been confirmed by the occurrence of two new peaks of (C=N) at 1614, 1632 along with the existence of above mentioned IR peaks with minute shifts (Fig. 2c) for the formation of LPOM-Sil-NH. In Fig. 2c presence of unaffected FT-IR bands for Keggin structure of LPOM confirmed its persistence even after modification of LPOM-Sil by covalent attachment of 2-hydroxy-1-naphthaldehyde. Fig. 3(a) shows the FT-IR spectrum of LPOM-Sil-NH-Cu which was recorded upto far infra-red region i.e. 300 for metalation of LPOM-Sil-HN. The FT-IR band at 448 is due to Cu-N stretching vibration which implies that copper has been coordinated through N of C=N and the band at 602 is due to stretching vibration of Cu-O bond which is the deprotonated –O-H- group of 2-hydroxy-1-naphthaldehyde.[17]. Fig. 3(b) shows the FT-IR bands of CS in which characteristic peak at 1636 corresponds to N-H bending vibration

(amines) and the peak at 1072 is due to the bridge oxygen (C-O-C) stretching vibration [14]. FT-IR spectrum of NH (Fig. 3c) exhibit broad peak - 3400 corresponding to –OH group and the peak at 1636 is due to N-H bend of $–NH_2$. Further, the presence of characteristic FT-IR peaks that have been present in CS and LPOM-Sil-NH-Cu is also present in NHyd with a minor shift which indicates the encapsulation of LPOM-Sil-NH-Cu into CS.

3.2 EDX and ICP Analysis

EDX study of nanohybrid have further confirmed that the stoichiometric ratio of W atom from LPOM and Cu atom present in NH is 11 atoms of W per 1 atom of Cu, further this analysis also proves the presence of all expected elements i.e. C, N, O in predictable ratio (Fig. 4). ICP study of NHyd further corroborated the results of EDX by exhibiting the presence of W, Si and Cu in the same amount as expected in the nanohybrid (Table 1), Calculated % Cu, 1.85; Si, 2.54; W, 61.97; found % Cu, 1.88; Si, 2.55; W, 61.52.

3.3. SEM Image of NHyd

Particle size and morphology of the nanohybrid has been characterized with Scanning Electron Microscope (SEM) imaging. A representative size distribution of NHyd is shown in Fig. 5. The particle size was found to be in the physiologically relevant range from 80-130 nm with an average around 110 nm as processed by Image J software.

The UV-Vis spectrum of LPOM (α-$K_8SiW_{11}O_{39}$) in DMSO (Fig. 6a) shows absorption band in the region 200 to 450 nm with peak at 209 and 265 which were attributed to the charge transfer transmission from O^{2-} to W^{6+} in Keggin type lacunary structure at W=O and W-O-W. The UV-Vis spectra of LPOM-Sil-NH-Cu is shown in Fig. 6b which shows that coordination geometry of Cu(II) ion may be tetrahedral

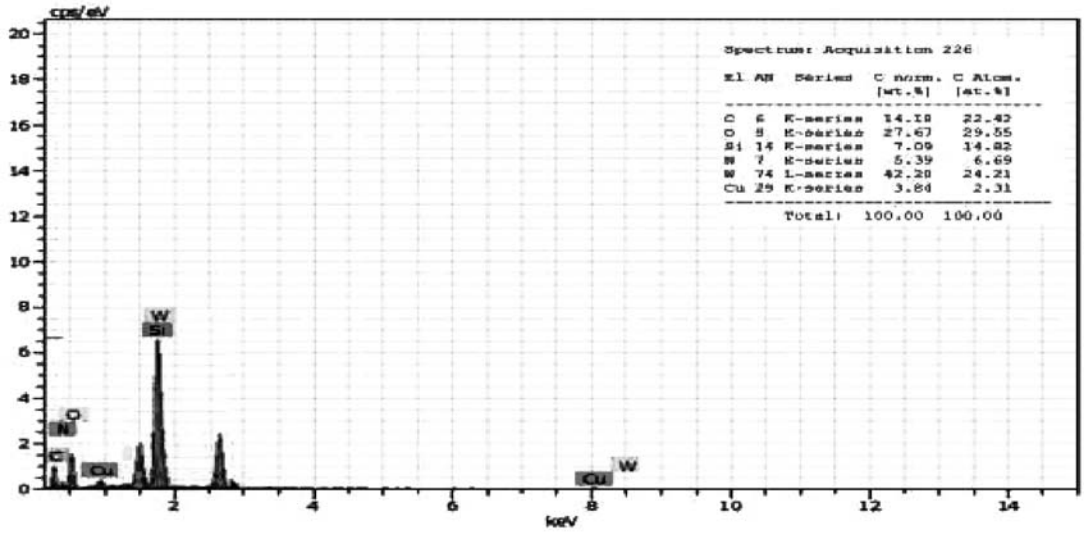

Fig. 4. EDX of NHyd

Table 1: ICP analysis of NHyd

	Concentration	Wavelength
Copper(Cu)	0.005 gm/L	327 nm
Tungsten(W)	0.126 gm/L	241 nm
Silicon(Si)	0.004 gm/L	255 nm

showing absorbance Cu(II) ion at 470 nm and 530 nm. The presence of two absorption peaks that were present in UV-Vis spectra of (α-$K_8SiW_{11}O_{39}$) with small shift in LPOM-Silane-2H1N-Cu indicate that organosilane was covalently linked to (α-$K_8SiW_{11}O_{39}$).

Firstly, UV-Vis spectra of LPOM-Sil-NH-Cu of known concentration was recorded (Fig. 7a). Then after four readings of UV-Vis spectra was taken during NH synthesis keeping the same concentration of LPOM-Sil-NH-Cu. First reading of supernatant was taken just after sonication

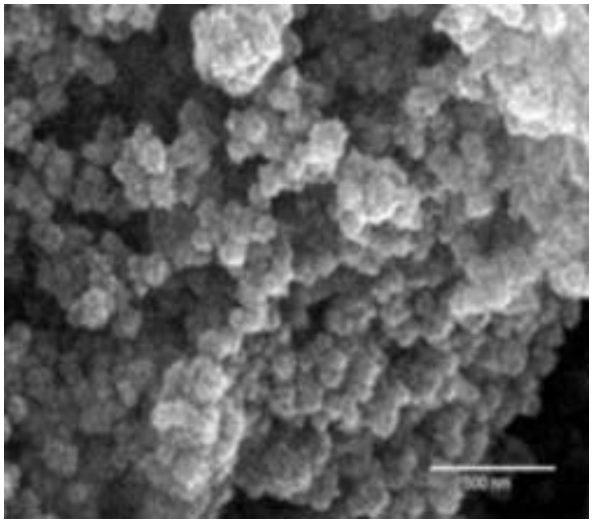

Fig. 5. SEM Image of NHyd

was stopped (Fig. 7b), second reading of supernatant was taken after two hours of continuous stirring of colloidal suspension of LPOM-Sil-NH-Cu and CS (Fig. 7c). Third reading was taken after ten hours of continuous stirring (Fig. 7d) and fourth reading of supernatant was taken after centrifugation (Fig. 7e). The first reading shows the presence of typical absorption peak of LPOM-Sil-NH-Cu and in second reading this peak got diminished which shows that LPOM-Sil-NH-Cu is entrapped into CS. The characteristic peaks of LPOM-Sil-NH-Cu finally vanished in the third and fourth reading of UV-Vis spectra. This clearly indicates that LPOM-Sil-NH-Cu was successfully encapsulated into CS after centrifugation [18].

3.5 Entrapment and Release of LPOM-Sil-NH-Cu from the NHyd

The loading and entrapment efficiencies of LPOM-Sil-NH-Cu within the NHyd were evaluated mathematically from the spectrophotometric data using the earlier mentioned formulae. The

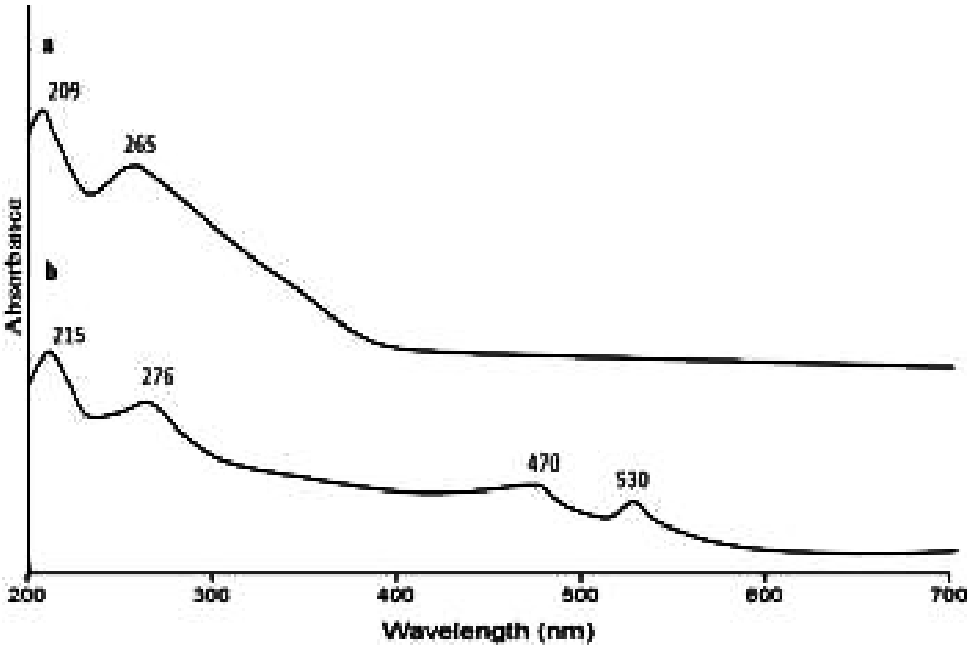

Fig. 6. (a) UV-Vis spectrum of LPOM (b) LPOM-Sil-NH-Cu

un-entrapped LPOM-Sil-NH-Cu remaining in the suspension was calculated by measuring the Optical Density (OD) of LPOM-Sil-NH-Cu in the supernatant. From the standard curve, the entrapment efficiency of POMs within the NHyd was evaluated to be 81.2% and loading efficiency was 59.1%. High drug loading and entrapment efficiency can be attributed to the electrostatic interaction between the cationic nanohybrid matrix and the LPOM-Sil-NH-Cu drug functional groups.

The release behaviour of LPOM-Sil-NH-Cu, was investigated in two different pH (7.4 and 5.0) of PBS, and the results is illustrated in Fig. 8. Based on the evidence, the environment of tumor tissues has a relatively lower pH due to the higher metabolism, and this condition is more common in the lysosomal area. Because of cationic pendant groups and other amine groups within the chitosan matrix, it was expected the prepared nanoparticle provide a response to the pH triggers and make the higher

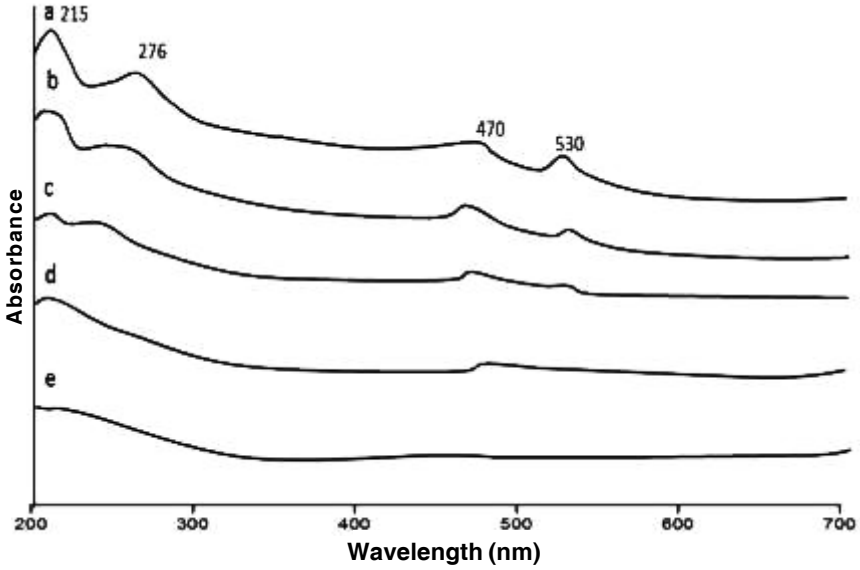

Fig. 7. UV Vis Spectra of (a) LPOM-Sil-NH-Cu (b) First Reading was taken just after sonication of NHyd was stopped (c) Second reading after two hours of continuous stirring of colloidal suspension of NHyd (d) Third Reading after ten hours of continuous stirring of colloidal suspension of NHyd (e) Fourth Reading was taken after centrifugation of NHyd

release profile [19]. As expected, the release of POMs from the prepared NHyd (Fig.7) shows a pH dependent behaviour. Release at a pH of 7.4 is slower than the acidic condition (pH=5.0). In the 12 h, about 48.6%, and 28.5% of the POMs has been released at pH of 7.4, and pH of 5, respectively. Totally, after 96 h, 89.2% of POMs has been released at acidic pH while only 50.2% at physiologic pH in a sustained manner. According to the significant difference between the LPOM-Sil-NH-Cu released percent at all times, the LPOM-Sil-NH-Cu with a pH-sensitive behaviour are an efficient system for delivery of this cytotoxic agent to the cancerous cells, especially at acidic conditions within the lysosome.

3.6 Antibacterial Activity

The antibacterial properties of LPOM-Sil-NH-Cu and NHyd have been tested against two bacterial strains *B. subtilis* gram (+ve) and *E. Coli* gram (–ve), the effect of LPOM-Sil-NH-Cu and NHyd (inhibitory zone) data are tabulated in Fig. 9. LPOM-Sil-NH-Cu shows potential antibacterial activity due to presence of copper ions against both bacterial strains. As evident from Fig. 9 that NHyd show potential antimicrobial activity against both gram (+)ve and (-)ve in comparison to bare LPOM-Sil-NH-Cu. The reason behind excellent activity might be due to interaction of positively charged amino groups in chitosan with the negatively charged phosphorous and sulfur compounds present in proteins and nucleic acid of bacteria, this result in structural changes and deformation of cell wall and cell membrane and ultimately leading

to cell death [6]. Enhanced antibacterial activity of the NHyd may also be attributed to its small size which can easily diffuse through membrane, hence affecting functioning of physiological activity of bacteria.

4. CONCLUSIONS

In the present CS and POM based nanohybrid were formulated by simple and robust ionotropic gelation technique. The prepared nanohybrid was characterized at each step by different characterization techniques. Spherical NHyd with an average size around 110 nm exhibited excellent loading and entrapment efficiency. Drug release study suggested their potential application for pH-dependent sustained release for tumor therapeutics. Antibacterial results also suggested their potential application for bacterial infections. Further, LPOM-Sil-HN-Cu can be studied by our research group for targeted treatment of tumor cells by drug delivery method. The above results suggest the potential applicability of the prepared nanohybrid for chemotherapeutic treatment of cancer. Additionally, it will also play an important role in combating other bacterial infections during the treatment process.

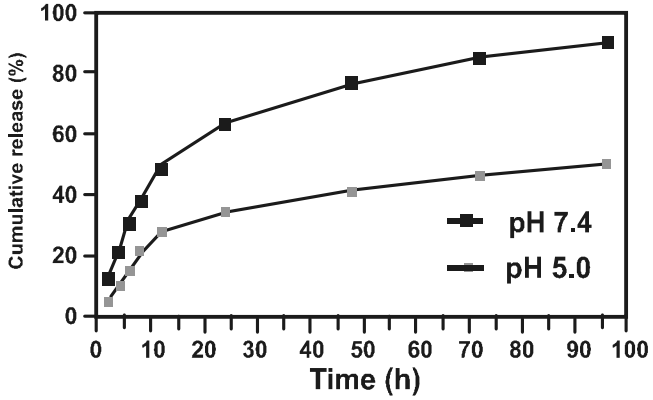

Fig. 8. Time dependent release study of POM from NHyd

Acknowledgement: One of the authors (SA) is grateful to Vice-chancellor, Dr. Shakuntala Misra National Rehabilitation University

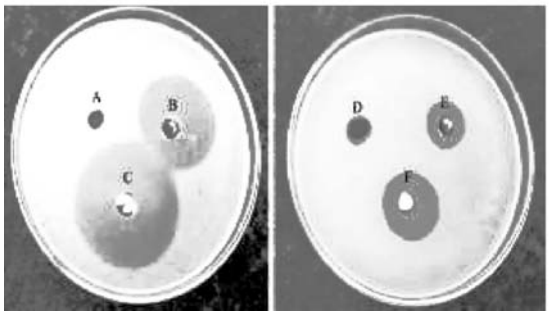

Sample		Zone of Inhibition (mm)
A (Control)	Against Gram Negative Bacteria (*E.Coli*)	NS
B (LPOM-Sil-HN-Cu)		29 ± 3
C (NHyd)		46 ± 1
D (Control)	Against Gram Positive Bacteria (*B.Subtilis*)	NS
E (LPOM-Sil-HN-Cu)		18 ± 1
F (NHyd)		23 ± 2

Fig. 9. Antibacterial assessment result against two different bacterial strains

Lucknow to provide him University-Post Doctoral Fellowship (2209/1466 DSMNRU Research Cell 2020-21, dated 18 January 2022) to carry out the research work.

References

1. P. K. Dutta, J. Dutta, M. C. Chattopadhyaya, V. S. Tripathi. (2004). *J. Polym. Mater.,* 21: 321-333.
2. (a) D. Archana, J. Dutta, P. K. Dutta. (2013). *Int. J. Biol. Macromol.* 57: 193-203. (b) D. Archana, B. K. Singh, J. Dutta, P. K. Dutta. (2015). *Int. J. Biol. Macromol.* 73: 49-57. (c) B. K. Singh, R. Sirohi, D. Archana, A. Jain P. K. Dutta. (2014). *Int. J. Polym. Mater. Polym. Biometar.,* 64: 242-252.
3. (a) S. F. Peng, M. T. Tseng, Y. C. Ho, M. C. Wei, Z. X. Liao, H. W. Sung, Biomaterials. (2011). 32, 239-248. (b) Q. Zhao, X. Feng, S. Mei, Z. Jin. (2009). *Nanotechnology,* 20: 105101.
4. D. L. Long, E. Burkholder, L. Cronin. (2007). *Chem. Soc. Rev.,* 36: 105-121.
5. (a) B. Hasenknopf, Front. Biosci. (2005). 10: 275 -287; (b) J. T. Rhule, C. L. Hill, D. A. Judd, R. F. Schinazi. (1998). *Chem. Rev.,* 98: 327-357; (c) S. Arun, P. Bhartiya, A. Naz, S. Rai, S.S. Narvi, P.K. Dutta. (2018). *J. Polym. Mater.,* 35 (4): 473-482; (d) M. Witvrouw, H. Weigold, C. Pannecouque, D. Schols, E. De Clercq, G. Holan. (2000). *J. Med. Chem.,* 43: 778-783; (e) S. Shigeta, S. Mori, T. Yamase, N. Yamamoto. (2006). *Biomed. Pharma.,* 60: 211-219.
6. S. Arun, V. K. Singh, A. Naz, P. K. Dutta. (2021). *J. Indian Chem. Soc.,* 98: 100118.
7. L. Zhang, J. M. Chan, F. X. Gu, J.-W. Rhee, A. Z. Wang, A. F. Radovic-Moreno, F. Alexis, R. Langer and O. C. Farokhzad. (2008). *ACS Nano,* 2: 1696-1702.
8. K. A. Whitehead, R. Langer and D. G. Anderson. (2009). *Nature Rev. Drug Discov.,* 8: 129-138.
9. F. Zhai, D. Li, C. Zhang, X. Wang, R. Li. (2008). *Eur. J. Med. Chem.,* 43: 1911-1917.
10. (a) M. Bonchio, M. Carraro, G. Scorrano, E. Fontananova, E. Drioli, Adv. Synth. Catal., 345 (2003) 1119 – 1126; (b) G. Geisberger, S. Paulus, M. Carraro, M. Bonchio, G.R. Patzke. (2011). *Chem. Eur. J.* 17: 4619-4625.
11. A. Teze, G. Herve. (1977). *J. Inor. Nucl. Chem.,* 39: 999.
12. I. Bar-Nahum, H. Cohen, R. Neumann. (2003). *Inorg. Chem.,* 42: 3677-3684.
13. S. Arun. (2018) . *Adv. Chem. App. Scien.,* ISBN: 978-81-9350520-5; Vol. 1: 133.
14. (a) D. Menon, R. T. Thomas, S. Narayanan, S. Maya, R. Jayakumar, F. Hussain, V. K. Lakshmanan, S. V. Nair. (2011). *Carbohyd. Polym.,* 84 , 887-893. (b) P. Bhartiya, R. Chawla, and P.K. Dutta. (2022). *Macromol. Chem. Phys.,* 223: 2200140.
15. P. Bhartiya, R. Chawla and P.K. Dutta. (2022). *J. Macromol. Sci.,* Part A, 59(12): 810-817.
16. P. Bhartiya and P. K. Dutta. (2018). *J. Polym. Mater.,* 35 (1): 85-101.
17. K. Helios, R. Wysokinski, A. Pietraszko, D. Michalska. (2011). *Vibra. Spectro.,* 55: 207-215.
18. A. Naz, S. Arun, S.S. Narvi, M.S. Alam, A. Singh, P. Bhartiya, P.K. Dutta. (2018). *Int. J. Biol. Macromol.,* 110: 215-226.
19. Shiva Arun, Y. Singh, A. Naz, P. Bhartiya, K. Srivastava, S. S. Narvi and P. K. Dutta. (2018). *J. Polym. Mater.,* 35 (3): 305-316.

Received: 21-01-2023

Accepted: 15-02-2023